Visual Abstract

Analysis of strengthened short deficient rubberized concrete-filled steel tubular columns

Fady A. Elshazly, Suzan A. A. Mustafa*, Hesham M. Fawzy
Zagazig University, Egypt
Fadiame@zu.edu.eg, https://orcid.org/0000-0002-4247-0874
samustafa@eng.zu.edu.eg, http://orcid.org/0000-0001-9647-2456
hesham_fawzy2000@yahoo.com https://orcid.org/0000-0003-3847-7384

ABSTRACT. Concrete-filled steel tubular (CFST) columns are broadly used in many structural systems for their well-known merits. This paper presents a finite element investigation on the structural behaviour of short circular deficient steel tubes filled with rubberized concrete (RuC), under axial compressive load. To accomplish this study, a validation of the proposed three-dimensional nonlinear finite element model; using ANSYS software; was carried out showing good accurateness. The analysis involved two different concrete mixes with 5% and 15% replacement of fine aggregate volume with crumb rubber particles. Columns strength reduction due to horizontal or vertical deficiencies was handled by increasing the thickness of the steel tube or wrapping the columns with two different types of FRP sheets. Five strengthening arrangements were studied using GFRP sheets and CFRP sheets. The results indicated that the ultimate bearing capacity of the RuCFST columns was increased with increasing the steel tube thickness. application of FRP sheets for strengthening the deficient RuCFST columns efficiently managed to retrieve the strength-lost due to either horizontal or vertical deficiency. Moreover, an enhancement in the columns' ductility was observed especially when using GFRP sheets.

KEYWORDS. Rubberized concrete; Axial compression; Deficiencies; RuCFST; FRP.

OPEN ACCESS

Citation: Elshazly, F. A., Mustafa, S. A. A., Fawzy, H. M., Analysis of strengthened short deficient rubberized concrete-filled steel tubular columns, Frattura ed Integrità Strutturale, 55 (2021) 1-19.

Received: 09.06.2020
Accepted: 20.09.2020
Published: 01.01.2021

INTRODUCTION

Structural engineering witness high rate of progress accompanied with high ambition to get the most benefit of all members consisting the structure. Members with high ultimate strength and small cross sections are needed to achieve structural and architectural requirements. One of the most important structural members is the column, that must attain the loads of the structure safely. Increasing loads in tall buildings need effective and economic design of columns. Composite columns can attain high loads with small cross section in comparison with concrete columns. One of composite

columns types is Concrete Filled Steel Tube (CFST) columns. In order to increase the capacity of this type to meet the requirements of loads increase or to rehabilitate deficient members, Fiber Reinforced Polymers (FRP) sheets can be used. FRP sheets can provide high confinement for the columns that leads to an increase in ultimate bearing capacity. Earthquakes are great concern that must be taken in structures design. Elements in seismic areas need high ductility. Ductility of CFST columns can be increased by using Rubberized Concrete (RuC) in which rubber is added to the concrete mix as a partial replacement of fine or coarse aggregate. Advantages of CFST and RuC can be gathered in Rubberized Concrete Filled Steel Tube (RuCFST) column. This column can attain high loads with high ductile behavior. Concrete core in this column type has a great rule in controlling the local inward buckling occurrence of the steel tube. Schneider [1] studied experimentally and analytically the behavior of short steel tubular columns filled with concrete under concentric compressive loads. He showed that columns with circular section had better behavior than square and rectangular sections. Circular sections provided substantial post-yield strength, ductility, and stiffness more than the other two sections. He proposed that effective confinement was achieved at 92% of yield strength. He elucidated that after reaching the yield load, square and rectangular sections did not provide sufficient confinement.

FRP can be used to wrap CFST column to provide effective confinement that leads to an increase in ultimate bearing capacity and local outward buckling delaying. Despite of FRP materials' high cost, they have several advantages that make their usage beneficial such as easy and rapid application and high provided confinement/thickness ratio in comparison with steel sections. FRP materials can be used in design of CFST column or CFST rehabilitation. Sundarraja and Prabhu [2] studied experimentally the behavior of steel tubes filled with concrete and partially wrapped with Carbon Fiber Reinforced Polymers (CFRP) under axial compressive loads. They showed that CFRP provided effective confinement, delayed local buckling occurrence, and increased ultimate bearing capacity in agreement with the results of Lu et al. [3] and the experimental and numerical results of Shen et al. [4]. They concluded that unwrapped areas exhibited strains increase that led to local buckling occurrence at these areas. Prabhu and Sundarraja [5] studied experimentally and analytically the effect of strengthening CFST using CFRP strips under compressive load. They strengthened the specimens using transversal CFRP strips. They outlined that CFRP strips using in external wrapping of CFST specimens was effective in delaying the local buckling of the CFST specimens. Increasing CFRP layers number increased the ultimate load of the columns depending of the CFRP strips spacing. Prabhu et al. [6] agreed with the previous results of Prabhu and and Sundarraja [5]. They [6] figured out that confinement was enhanced with the increase in CFRP layers. They proposed that using CFRP strips in strengthening of CFST columns at spacing of 20 mm or 30 mm would be so effective. They preferred using spacing of 30 mm according to economical view. Alam et al. [7] studied CFST specimens with and without FRP strengthening under drop hammer impact. They observed that lateral displacement of CFST members could be reduced up to 18.2% by using FRP sheets. They outlined that CFRP sheets, in case of wrapping in longitudinal direction, were weak under impact load. They proposed that using CFRP or GFRP sheets combination in both longitudinal and transversal directions could help in minimizing FRP damage under lateral impact load. Deng et al. [8] Studied experimentally axial compressive capacity of CFST specimens confined with CFRP and Basalt Fiber Reinforced Polymers (BFRP). They elucidated that using CFRP and BFRP enhanced the axial compressive capacity up to 61.4% and 17.7%, respectively. Liu et al. [9] studied experimentally and theoretically the axial static behavior of circular stub composite tubed concrete columns confined using CFRP. They observed high confinement of CFRP that caused an increase in ultimate load even after steel tube yielding. They proposed that specimens strengthened using CFRP exhibited better ductile behaviour compared to bare specimens. Na et al. [10] investigated the effect of slenderness ratio on the behaviour of CFST columns strengthened using CFRP. They showed that transversal wrapping using CFRP enhanced the columns behaviour effectively. This enhancement decreased with the increase in slenderness ratio. Reddy and Sivasankar [11] studied the effect of GFRP sheets strengthening on the behaviour of corroded CFST columns. They showed that GFRP sheets were effective in delaying local buckling and increasing compressive strength. The failure mode was mainly by GFRP sheets rupture. They outlined an increase in ultimate compressive load of columns wrapped with one, two and three GFRP layers up to 5.32%m 8.41% and 10.19%, respectively, compared to bare specimens. Cao et al. [12] studied experimentally the behaviour of Ultra-High Performance Fiber-Reinforced Concrete (UHPFRC) in CFST confined with FRP under axial compressive load. They outlined enhancement in ultimate bearing capacity of the specimens due to confinement provided by FRP. The enhancement level was higher in case of circular cross-sections compared to rectangular cross-sections. The main failure mode was mainly FRP rupture at corners in case of rectangular cross-sections and at the mid-height in case of circular cross-sections. Increasing GFRP or CFRP layers increased the confinement effectiveness. Tang et al. [13] studied Concrete-Filled Stainless Steel Tube (CFSST) stub columns confined using FRP under axial load. They showed that the main failure mode was by CFRP rupture at mid-height. They proposed an enhancement in ultimate load capacity up to 71.35% depending on CFRP layers. They observed an improvement in energy absorption due to CFRP provided confinement.

Several ways are available to upgrade columns and enhance their capacity. One of the most effective ways is using FRP sheets to strengthen columns. Several studies were performed to analyze this case by adding deficiencies to columns and strengthening them using FRP sheets. Ghaemdoust et al. [14] studied experimentally and numerically deficient short steel tubular columns wrapped with CFRP sheets. The specimens had initial horizontal or vertical deficiencies. Karimian et al. [15] studied deficient hollow circular steel tubes with initial deficiencies in transversal or longitudinal directions and strengthened with CFRP under axial compressive loads. They [14, 15] showed that there was a loss in ultimate bearing capacity because of deficiencies occurrence. They [14, 15] proposed that using CFRP sheets compensated effectively this loss. Number of CFRP layers had significant effect on confinement effectiveness, gain in ultimate bearing capacity, delaying local buckling occurrence and decreasing stress concentration at the deficiency location.

Concrete mixes' properties depend on the materials composing the mix. Several materials can enhance the properties of concrete mixes. Adding rubber to concrete mixes that scientifically named Rubberized Concrete (RuC) can enhance the mix ductility, Fawzy et al. [16]. Several researchers studied the behavior of RuC. Jiang et al. [17] studied experimentally specimens of steel tubes filled with rubberized concrete and normal concrete to analyze the differences in the behaviour of the two types. A number of 36 specimens were tested experimentally. All specimens were tested under cyclic and monotonic lateral loads with normalized axial loads at several levels. The results showed that the concrete core provided efficient restraining of steel tubes against occurrence of local buckling. Thus, preventing premature failure that might occur due to local buckling. It was observed that the concrete damage controlled the ductility of the specimens. The cross-section slenderness had a great effect on the occurrence of the concrete damage which in turn influenced the ductility of the specimen. Duarte et al. [18] studied short steel tubular columns filled with rubberized concrete. They showed that specimens with rubberized concrete exhibited lower strength under compression and tension and higher ductile behaviour in comparison with normal concrete specimens. They proposed that in case of specimens with circular section, confinement effectiveness decreased with the increase in rubber content. This effect was a result of concrete core crushing after the tube initiated to buckle, and as a result of lower dilation angle of rubberized concrete in comparison with normal concrete. Abendeh et al. [19] studied the behavior of steel tubes filled with rubberized concrete. They showed that increasing rubber content led to a decrease in compressive strength. They elucidated that the bond in case of circular cross sections was higher than square cross sections. Elchalakani et al. [20] studied experimentally short columns composed of circular steel tubes with double skin and filled with rubberized concrete with different contents of rubber in the concrete mix. The results showed that the ultimate compressive strength in case of rubberized concrete with 15% and 30% rubber content was lower than that of normal concrete mix by 50% and 79%, respectively. The results showed that adding of rubber to the concrete increased the ductility of the concrete filled steel tube up to 250 %. Dong et al. [21] studied rubberized CFST (RuCFST) to investigate the effect of confinement provided by the steel tube to the RuC core on specimens' ductility and strength. They proposed that rubber existence in concrete caused strength decrease and ductility increase of the concrete mix. They showed that this strength reduction was effectively overcome by the steel tube confinement. RuCFST specimens had better ductile behavior compared to normal CFST specimens. They outlined that high ductility of RuC led to well bond between the concrete core and the steel tube. The RuC core deformed and filled the buckles. RuCFST specimens had higher energy absorption compared to normal CFST specimens.

The main aim of this paper is to present a three-dimensional nonlinear finite element model using ANSYS [23] software to simulate the RuCFST short columns under axial compressive load. The model simulated the behaviour of the RuCFST columns and its accuracy was proven using twenty experimentally tested specimens from literature. The overall behaviour of the RuCFST deficient columns was studied, in addition to studying the effect of increasing the steel tube thickness and strengthening the columns with FRP sheets to retain the lost strength.

FINITE ELEMENT MODELING

General

A three-dimensional nonlinear finite element model was proposed to investigate the behavior of deficient short RuCFST columns under axial compressive load. Some of these columns were strengthened using FRP sheets. All the components of the specimens such as steel, concrete core and FRP sheets had to be modeled properly. In addition, the interface between steel tube and the concrete core had to be modelled carefully, to accurately simulate the real behaviour of the studied columns. ANSYS [22] software was utilized to perform the nonlinear Finite Element Analysis (FEA) of the specimens. Choosing the appropriate element type and mesh size controls the accuracy and the computational time needed for accurate results. The proposed finite element model was verified by using seventeen specimens tested by the authors in addition to other research data available from literature.

Finite element type and mesh

ANSYS [22] library provides several types of elements to simulate various structural elements with high accuracy. Each element has its own properties. Mesh sizes have to be determined accurately to obtain precise solution with acceptable solution time. The desired mesh size ratio; 1:3; was considered for accurate results. A three-dimensional 8-node solid element SOLID65 was used to simulate concrete elements. This element is used in 3-D modeling of solids in cases of using or not using reinforcing bars. It has the capability of cracking in tension and crushing in compressive stresses. Each node of its eight nodes has three transitional degrees of freedom in X, Y and Z directions. To model the steel tube and the steel loading plates, a three-dimensional 8-nodes solid element SOLID185 was used. Each node of its eight nodes has three transitional degrees of freedom in X, Y and Z directions. This element has the capability of stress stiffening, large deflections, large strain and creep. The different types of FRP sheet were modelled using a 4-node SHELL181 element. It has six degrees of freedoms at each node; three transitional degrees of freedom in X, Y and Z directions and three rotational degrees of freedom about X, Y and Z axes. It is well-suited for layered materials analysis. The interface between the different components of the CFST columns was modelled as frictional contact, which affirmed friction provided that the two surfaces remain in contact. Moreover, it inhibits physical penetration between the contacted components during the different loading steps.

Material modeling

For the sake of accuracy of the proposed model, the material properties of each component were considered as existed in the experimental work. One of the most important aspects is the stress-strain relation of concrete. The concrete compressive strengths in the finite element analysis were obtained from the experimental data from Elshazly et. al [23] and Duarte et al. [18] for the different simulated specimens. A typical shape of the concrete stress-strain relation is shown in Fig. 1 (a). The ascending branch of the stress-strain relationship followed Eqn. (1) and Eqn. (2) proposed by Liang and Fragomeni [24] and Liang [25] & [26]. In all studied specimens, the D/t ratio of the used steel tubes ranged from 32 to 50. These values provide remarkable confining for the concrete core. The model ignored the descending branch of the relationship to avoid the convergence problems in the finite element analysis solution. The confined compressive strength in circular concrete filled steel tubes of each concrete mix and ultimate confined strain were calculated using Eqn. (3) and Eqn. (4) proposed by Mander et al. [27], with the strength reduction factor γ_c proposed by Liang [26].

$$\sigma_c = \frac{f'_{cc}\ \lambda\left(\varepsilon_c / \varepsilon'_{cc}\right)}{\lambda - 1 + \left(\varepsilon_c / \varepsilon'_{cc}\right)^{\lambda}} \tag{1}$$

$$\lambda = \frac{E_c}{E_c - \left(f'_{cc} / \varepsilon'_{cc}\right)} \tag{2}$$

$$f'_{cc} = \gamma_c f' + k_1\ f_{rp} \tag{3}$$

$$\varepsilon'_{cc} = \varepsilon'_c \left(1 + k_2 \frac{f_{rp}}{\gamma_c\ f'_c}\right) \tag{4}$$

$$\upsilon_{RuC} = \upsilon_{NC} V_{concrete} + \upsilon_{rubber} V_{rubber} \tag{5}$$

where f'_{cc} refers to the confined compressive strength of the concrete, ε'cc refers to the strain at f'_{cc}, f_{rp} refers to the lateral confining pressure on the concrete core presented by Eqn. (3), f'_c refers to the unconfined compressive strength based on the experimental results, ε'_c refers to the strain at f'_c as illustrated by Tang et al. [28] and Hu et al. [29]. k_1 and k_2 were taken as 4.1 and 20.5, respectively based on the results proposed by Richart et al. [30]. The Poisson's ratio of the rubberized concrete mixes was calculated using Eqn. (5) provided by Duarte et al. [31], in which ν_{RuC} is the Poisson's ratio of rubberized concrete. $V_{concrete}$ and V_{rubber} are the volumetric fraction of the concrete mix and the rubber particles, respectively. ν_{NC} is the Poisson's ratio of normal concrete mix and was taken as 0.2, and ν_{rubber} is the Poisson's ratio of the rubber particles that was taken as 0.5. Using the aforementioned equations, confined compressive strength of concrete

mixes were calculated. Confined compressive strengths for NC, RU5 and RU15 were 59.6 MPa, 56 MPa and 51.5 MPa, respectively. Confined ultimate strain of NC, RU5 and RU15 was 0.00753, 0.00780 and 0.008268, respectively. Open shear transfer coefficient was taken as 0.4 and closed shear transfer coefficient was taken as 0.8. Uniaxial cracking stress was taken as 5.96 MPa, 5.6 MPa and 5.15 MPa for NC, RU5 and RU15, respectively. The steel properties were considered as the recorded experimental data in Tab. 1 which lists the yield stress; ultimate stress; yield strain; ultimate strain and the elastic modulus. Steel Poisson's ratio was assumed as 0.3 while the elastic modulus was 200 GPa. Fig. 1(b) shows a typical shape of the utilized steel stress-strain relationship.

Some specimens tested by Elshazly et al. [23] were strengthened using different types of FRP sheets. The FRP material was defined using linear elastic behavior with Poisson's ratio of 0.35. CFRP sheet had a thickness of 0.129 mm with ultimate tensile strength of 3500 MPa, ultimate strain of 1.56% and modulus of elasticity of 225 GPa. GFRP sheet had a thickness of 0.168 mm with ultimate tensile strength of 1500 MPa, ultimate strain of 2.14% and modulus of elasticity of 70 GPa as existed in the experimental work.

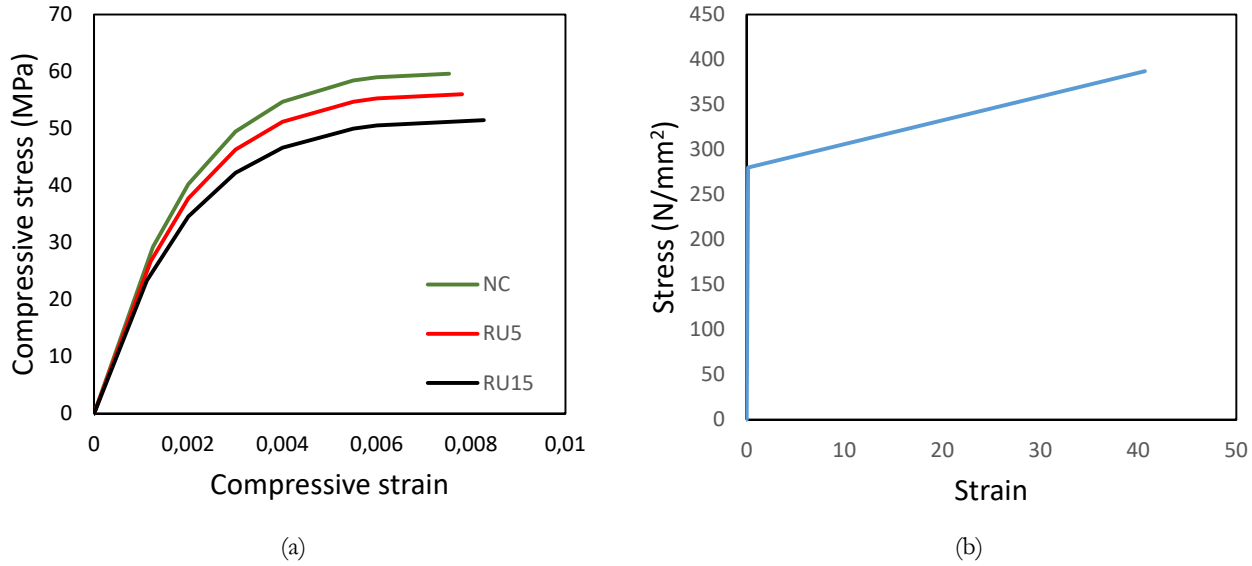

(a) (b)

Figure 1: Typical Stress-strain relation; (a) Concrete, (b) Steel.

	f_y (MPa)	f_u (MPa)	ε_y (%)	ε_u (%)
Elshazly et. al [23]	280	387	0.14	40.67
Duarte et al. [18]	310	400	0.14778	24

Table 1: Material properties of steel tubes.

Boundary conditions and load application

The test procedure performed by Elshazly et. al [23] and Duarte et al. [18] was imitated in the finite element analysis. Two loading plates were positioned at the top and the bottom of the specimens to insure a uniform distribution of the load. The load was applied at the centroid of the upper plate in Y direction. The top surface of the loading plate was restrained against any horizontal translation. The contact between the loading plates and CFST column components was fully bonded. The contact between the steel tube and concrete core was frictional contact with factor of friction 0.4, while the contact between the steel tube and the FRP sheets was fully bonded contact. The bottom surface of the specimen was restrained against any translation or rotation in all directions. Contact surfaces and load application of the proposed models are shown in Fig. 2. The load was applied as static axial load with small increments identical to the experimental investigations. Non-linear controls were by setting Newton-Raphson to program controlled option with force convergence criteria. The convergence tolerance limit was taken as 0.5% to achieve convergence of the solutions.

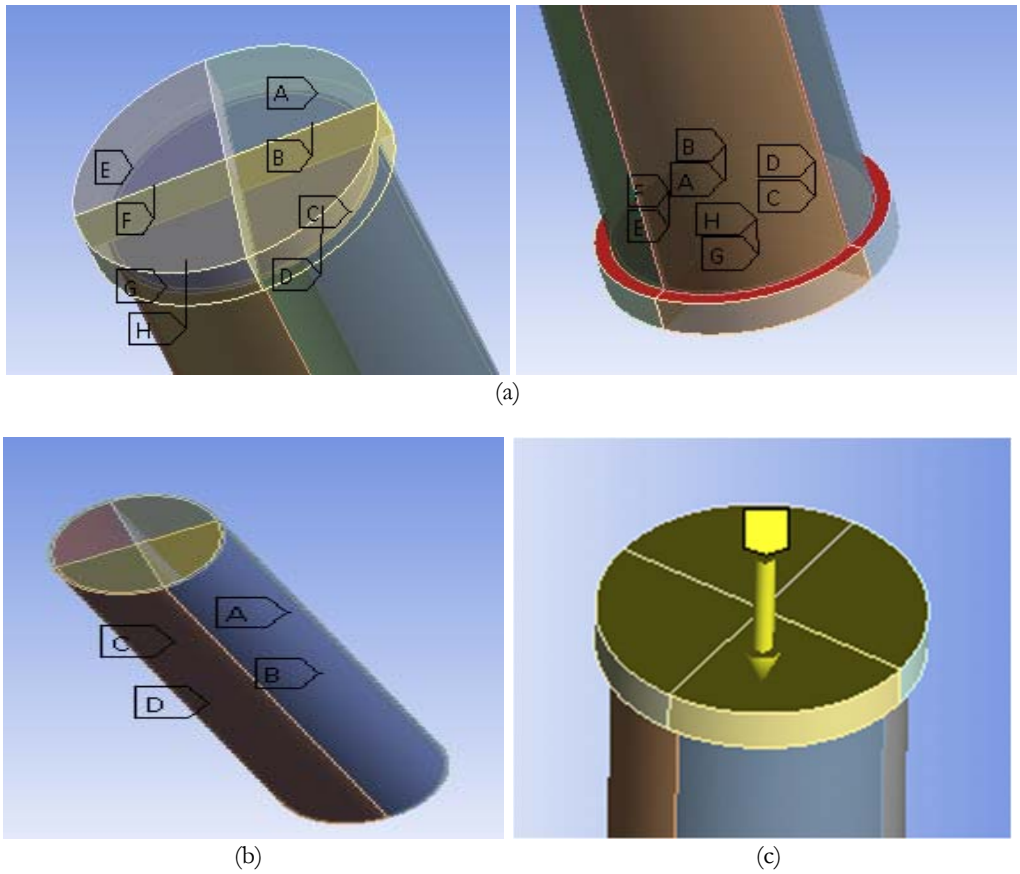

Figure 2: Loading and contact surfaces of the proposed model; (a) Contact between loading plates and CFST column components, (b) Contact between steel tube and concrete core, (c) Load application.

FINITE ELEMENT MODEL VALIDATION

Seventeen CFST columns tested by the authors in addition to three columns tested by Duarte et. al. [18], were simulated to verify the proposed finite element model. Specimen dimensions, material properties, boundary conditions and loading schemes were considered carefully from the experimental tests for the sake of accuracy, as detailed above. The comparison depended mainly on the ultimate load, load-axial shortening behaviour, deformed shapes and modes of failure.

Specimens tested by Elshazly et al. [23]

A wide range of parameters were considered in the seventeen specimens tested by Elshazly et al. [23], as detailed in Tab. 2. They examined non-deficient and deficient short RuCFST columns under axial compressive load. They used three concrete mixes; normal concrete (NC) with zero rubber content; rubberized concrete mix with 5% fine aggregate replacement with rubber particles by volume (Ru5); and rubberized concrete mix with 15% fine aggregate replacement with rubber particles by volume (Ru15). All specimens were 500 mm in length. The steel tube outer diameter was 125 mm and the thickness was 2.5 mm. The total length to external diameter ratio (L/D) was 4 for all specimen. The external diameter to thickness ratio (D/t) of the steel tubes was 50. Deficiencies were manufactured in some specimens in either longitudinal or transversal directions. Longitudinal deficiency had 300 mm length and 20 mm width. Transversal deficiency had a length of 100 mm and a width of 20 mm. Deficient specimens were strengthened using CFRP or GFRP sheets with different number and orientation of layers.

Specimen	L	D	T	Concrete		Deficiency			Strengthening			Ref.
	mm	mm	mm	Rubber %	f_{cu} MPa	Orien-tation	Length (mm)	Width (mm)	type	NT	NL	
NC	500	125	2.5	0%	41.7	---	---	---	---	---	---	Elshazly et al [23]
RU5	500	125	2.5	5%	38	---	---	---	---	---	---	
RU5-HL	500	125	2.5	5%	38	T	100	20	---	---	---	
RU15	500	125	2.5	15%	33.3	---	---	---	---	---	---	
RU15-HL	500	125	2.5	15%	33.3	T	100	20	---	---	---	
RU5HL-C1T	500	125	2.5	5%	38	T	100	20	CFRP	1	---	
RU5HL-G1T	500	125	2.5	5%	38	T	100	20	GFRP	1	---	
RU5HL-G1T1L	500	125	2.5	5%	38	T	100	20	GFRP	1	1	
RU5VL-C1T	500	125	2.5	5%	38	L	300	20	CFRP	1	---	
RU5VL-G1T	500	125	2.5	5%	38	L	300	20	GFRP	1	---	
RU5VL-G2T	500	125	2.5	5%	38	L	300	20	GFRP	2	---	
RU5VL-G1T1L	500	125	2.5	5%	38	L	300	20	GFRP	1	1	
RU15HL-C1T	500	125	2.5	15%	33.3	T	100	20	CFRP	1	---	
RU15HL-G1T	500	125	2.5	15%	33.3	T	100	20	GFRP	1	---	
RU15HL-G2T	500	125	2.5	15%	33.3	T	100	20	GFRP	2	---	
RU15VL-G2T	500	125	2.5	15%	33.3	L	300	20	GFRP	2	---	
RU15VL-G1T1L	500	125	2.5	15%	33.3	L	300	20	GFRP	1	1	
C114*3-235-0	300	114	2.7	0%	49.5	---	---	---	---	---	---	Duarte et al [18]
C114*3-235-5	300	114	2.7	5%	39.3	---	---	---	---	---	---	
C114*3-235-15	300	114	2.7	15%	25.2	---	---	---	---	---	---	

T: Transversal; NT: No. of layers in transversal direction; L: Longitudinal; NL: No. of layers in longitudinal direction

Table 2: Details of verified specimens.

To validate the proposed finite element model, the obtained results were compared to the experimental results. Axial load-axial shortening relations of the finite element results were plotted against experimental results in Fig. 3. Good agreement was noticed in the compared relations, not only in the initial stiffness but also in the ultimate strength. The mean value of the ratio between the ultimate experimental load and the corresponding Finite Element (FE) ultimate load, as detailed in Tab. 3, was about 0.988, with a corresponding coefficient of variation of about 0.026. However, the mean value of the ratio between the recorded axial shortening in the experimental results and their FE counterparts was about 0.89. The difference was due to the low deformation recorded in some experimentally tested specimens while the other specimens showed similar behaviour. Modes of failure in both cases were compared as well. Some examples of the compared specimens at failure are shown in Fig. 4. In case of bare deficient specimens, failure occurred at the deficiency location. This location exhibited high stresses and strains concentration. With increasing the load, warning notices appeared telling that the concrete core initiated to crush specially at deficiency location. When the specimen reached its ultimate bearing capacity, the deficiency location witnessed concrete crushing accompanied with high deformation in the steel tube. In specimens with transversal deficiency, the width of the deficiency initiated to decrease with increasing the load, as shown in Fig. 4. While in case of longitudinal deficiency, the width initiated to increase with increasing the load. In both cases, the edges of the deficiency started to buckle outward accompanied with concrete crushing at the deficiency location. In strengthened deficient specimens, the existence of FRP sheets postponed the local outward buckling in both cases of deficiencies. When the FRP sheets reached their ultimate strain, failure notice of the FRP sheet appeared. This failure was at the deficiency location followed by different other locations. Some of these failure modes from the finite element models which agrees with the modes of failure noticed in the experimental tests are shown in Fig. 4. The figure shows the finite element specimens' deformed shape attached with stress or strain values to clarify the most stressed and strained locations of the specimens. These values showed good accuracy in identifying the predicted failure position with good agreement with experimental results. Strain values were in mm/mm, while stress values were in MPa, as shown in Fig.4.

Specimens tested Duarte et al. [18]

Three concrete filled steel tubular columns with circular cross section under axial compressive load were modeled using the same presented technique. All the specimens had a length of 300 mm. The steel tube had a circular cross section with 114 mm outer diameter and 2.7 mm thick. The total length to external diameter ratio (L/D) was 2.63 for all specimen. The external diameter to thickness ratio (D/t) of the steel tubes was 42.2. The three specimens had three different concrete mix properties, as detailed in Tab. 2. The first concrete mix was normal concrete (NC) without any rubber content (specimen

C114*3-235-0), the second concrete mix was rubberized concrete with 5% replacement of the total aggregate content with rubber (RU5) (specimen C114*3-235-5) and the third mix was rubberized concrete with 15% replacement of the total aggregate content with rubber (Ru15) (specimen C114*3-235-15).

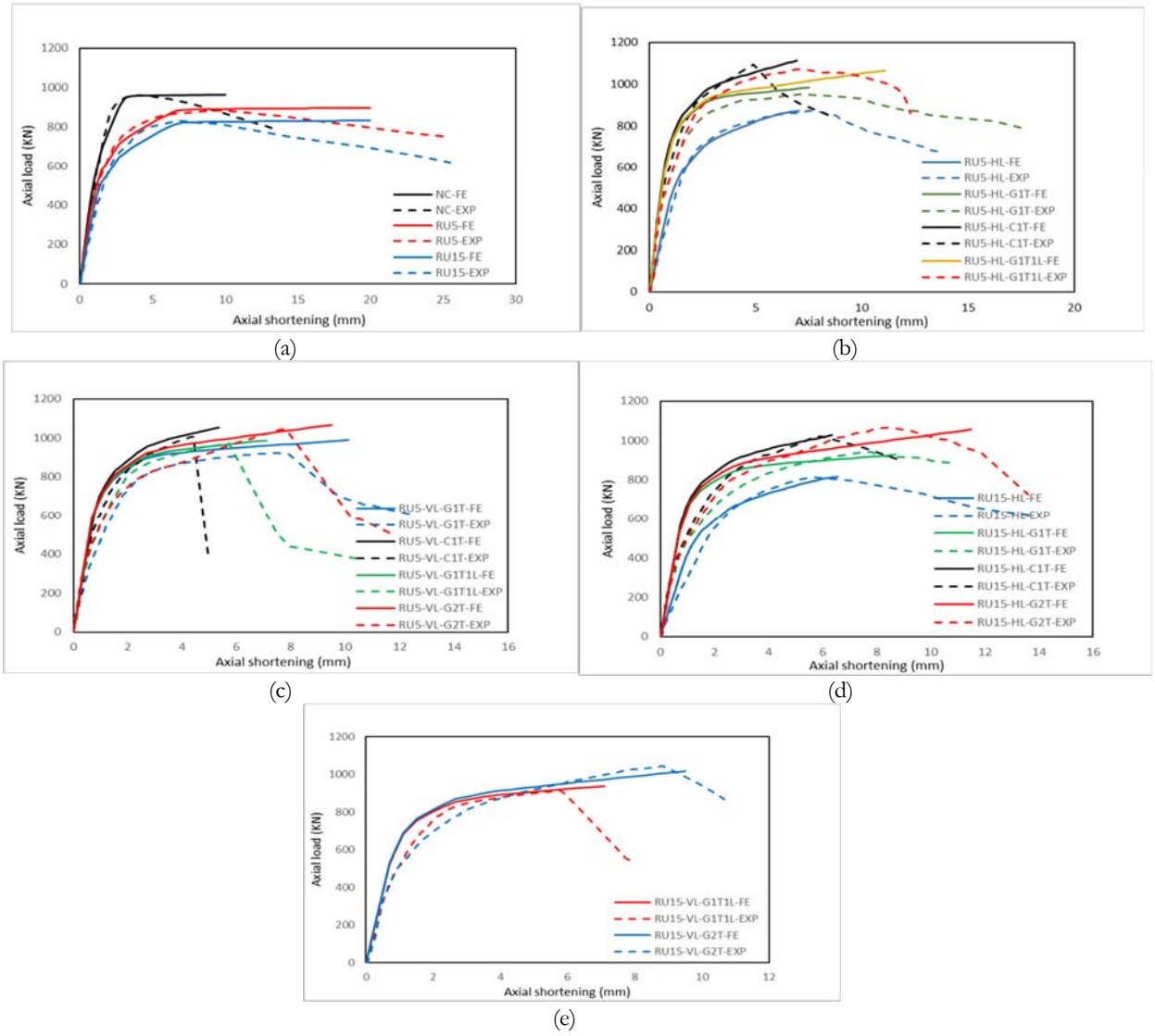

Figure 3: Load-axial shortening curves of proposed finite element model and experimental results; (a) Reference bare specimens, (b) Specimens with 5% rubber content and Hl deficiency, (c) Specimens with 5% rubber content and Vl deficiency (d) Specimens with 15% rubber content and Hl deficiency (e) Specimens with 15% rubber content and Vl deficiency.

A comparison between the results of the FE and the experimental results was carried out. Very good agreement in the results was noticed between the results. The proposed finite element model predicted both the ultimate load and the load-axial deformation relation efficaciously, as shown in Fig. 5 and Tab. 3. The mean value of the ultimate load ratio ($P_u(Exp)/P_u(FE)$) was about 0.97 while the COV of these results was about 0.015. The corresponding axial deformation ratio $(\Delta u(Exp)/\Delta u(FE))$ showed good results as well. The mean value was about 0.99 while the COV was about 0.053. These values indicate good accuracy of the proposed finite element model. Perfect match was noticed between the finite element analysis and the experimental counterpart until a load of about 400kN, shown in Fig. 5 (a, b, c). The axial shortening increased until the occurrence of local buckling in steel tube at mid-height of the columns, as shown in Fig. 5(d). High strain in the steel tube at the location of local buckling was observed which agreed with the deformed shape of the experimental specimen. The ultimate loads from the experimental and the finite element results of the twenty simulated columns were plotted in Fig. 6. The figure shows the accuracy and the reliability of the proposed finite element model to study the effect of some parameter to enhance the RuCFST columns behaviour.

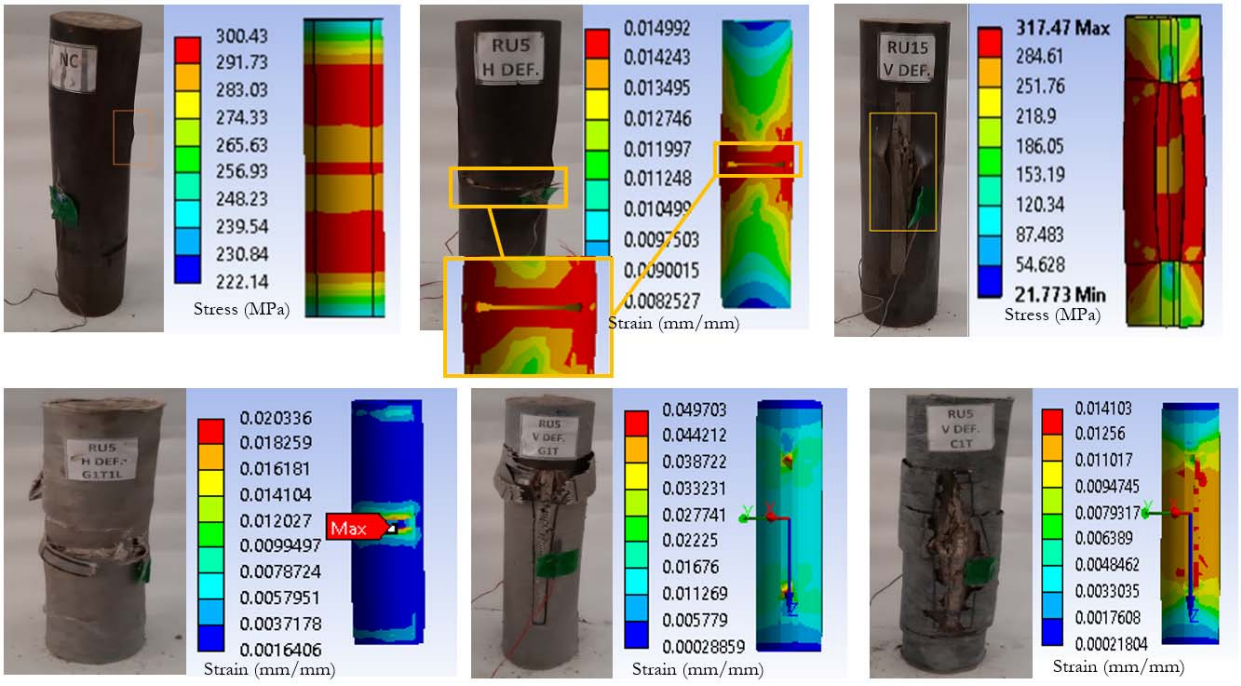

Figure 4: Failure shapes, stress and strain values of finite element models

Specimen	$P_{u(EXP)}$	$P_{u(FE)}$	$\frac{P_{u(EXP)}}{P_{u(FE)}}$	$\Delta_{u(EXP)}$	$\Delta_{u(FE)}$	$\frac{\Delta_{u(EXP)}}{\Delta_{u(FE)}}$	Ref.
NC	960	958	1.002	4.57	4.55	1.004	Elshazly et al [23]
RU5	884	887	0.996	9.21	7.1	1.29	
RU5-HL	874	870	1.005	7.7	7	1.1	
RU15	833	824	1.01	6.8	7.5	0.906	
RU15-HL	812	816	0.995	5.72	6.5	0.88	
RU5HL-C1T	1094	1113.9	0.982	4.9	6.95	0.705	
RU5HL-G1T	952	983.8	0.968	7.17	7.5	0.956	
RU5HL-G1T1L	1073	1066.2	1.006	7.1	11.1	0.639	
RU5VL-C1T	1007	1093.7	0.921	4.45	5.35	0.83	
RU5VL-G1T	923	971	0.95	8	9.8	0.816	
R	1045	1066.6	0.98	7.85	9.5	0.826	
RU5VL-G1T1L	972	988	0.984	5.73	7.1	0.807	
RU15HL-C1T	1020	1026.4	0.994	6	6.35	0.945	
RU15HL-G1T	942	927	1.016	7.66	8.7	0.88	
RU15HL-G2T	1066	1055.3	1.01	8.5	11.4	0.745	
RU15VL-G2T	1042	1017	1.02	8.85	9.5	0.932	
RU15VL-G1T1L	911	937.8	0.971	5.6	7.1	0.788	
C114*3-235-0	723.5	732.8	0.987	5.48	5.75	0.953	Duarte et al [18]
C114*3-235-5	595	617.5	0.964	8.8	8.95	0.983	
C114*3-235-15	482	501.5	0.961	10.3	9.75	1.056	

Table 3: Comparison between test results and FE model results.

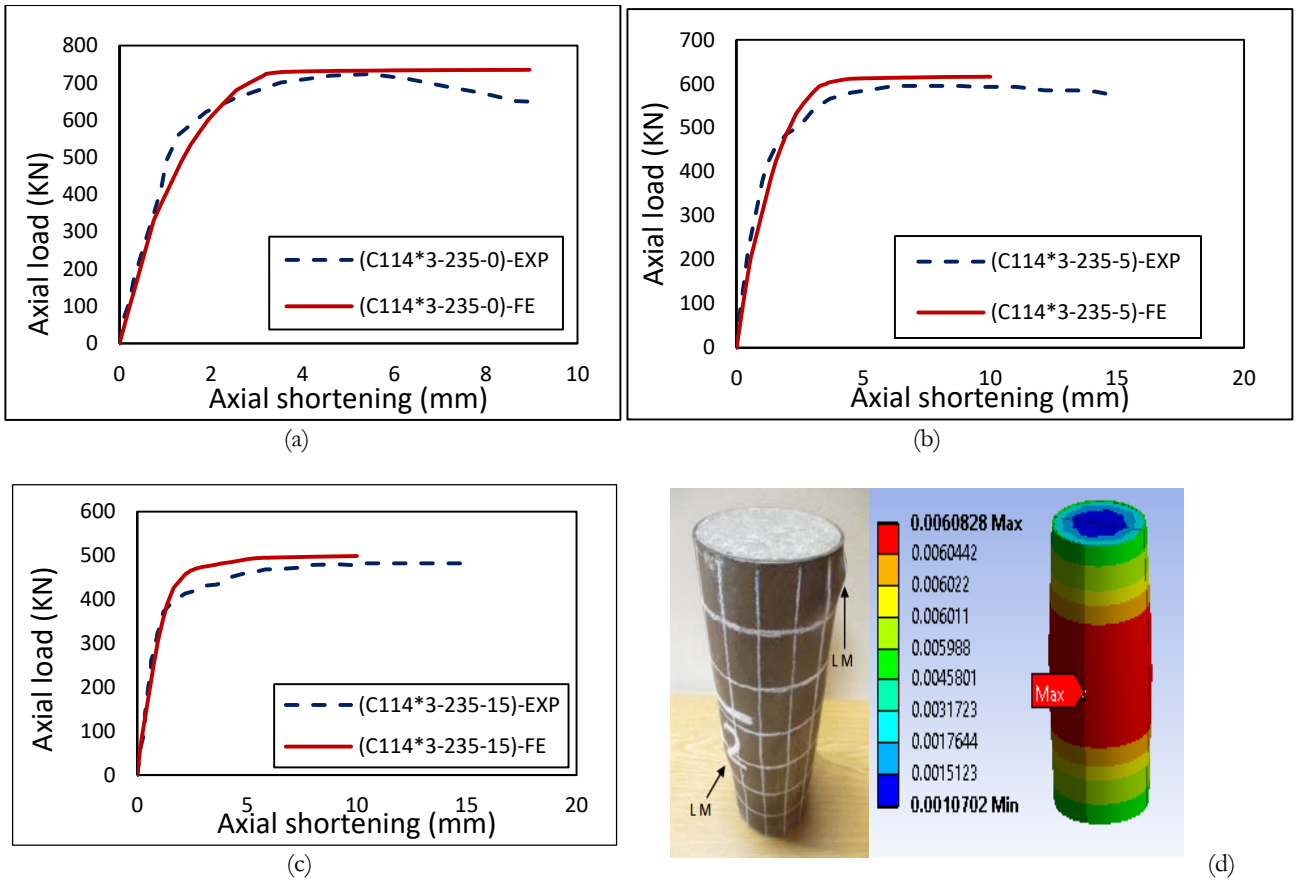

Figure 5: Comparison between proposed model and experimental results of Duarte et al. [18]; (a), (b), (c) Load-axial shorteing curves (d) Deformed shape at failure.

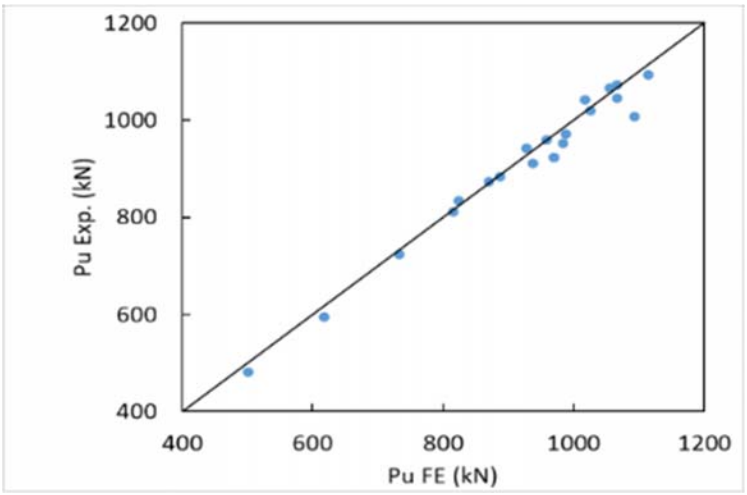

Figure 6: Experimental and finite element ultimate load of the twenty simulated CFST columns.

PARAMETRIC STUDY AND DISCUSSION

Sixty-four columns were analyzed using ANSYS program to investigate the influence of some parameters on the structural behaviour of the RuCFST columns. The studied parameters involved the rubber percentage included in the concrete mix design, the thickness of the steel tube, direction of manufactured deficiency, the type of the FRP sheets used in strengthening the deficient specimens in addition to the number and the direction of the used FRP sheets. The column dimensions, material properties and the sizes of the vertical and horizontal deficiencies were considered as tested by Elshazly et al. [23] which were listed in Tab. 1 and Tab. 2. The studied parameters are detailed in Tab. 4. The label of each column indicates the analyzed parameters. As an example (RU5-HL-C1T1L-T2.5): "RU" stands for rubberized concrete, "5" stands for rubber content of 5% as replacement of fine aggregate content, "HL" stands for horizontal (or transverse) deficiency, "C" stands for CFRP sheets, "1T" refers to one layer of FRP sheet in transversal direction, "1L" refers to one layer of FRP sheet in longitudinal direction and (T2.5) refers to the thickness of the steel tube. All the studied specimens had D/t ratios were chosen to be less than 125/ (f_y/250); according to Bradford et al. [32] to prevent local buckling.

Diameter to Thickness Ratio

Diameter to thickness D/t ratio may be either due to increasing the tube diameter or due to decreasing the tube's thickness. In this study, the analysis was carried out by keeping the diameter of the tubes constant and the thickness was varied. Twenty-four circular CFST columns were employed herein to explore the effect of this parameter on the column behaviour. The used steel tube thicknesses were 2.5, 3, 3.5 and 4 mm. This caused the D/t ratio to vary from 32 to 50 as illustrated in Tab. 4. These twenty-four columns were analyzed in six groups, each group contained four specimens with the four different studied tube thicknesses. The first group contained columns with rubberized concrete with 5% rubber content. The second group contained columns with rubberized concrete with 15% rubber content. The third and fourth groups had specimens with horizontal deficiency, while the fifth and sixth groups had specimens with vertical deficiency, with the afore-mentioned two concrete mixes.

It is worth pointing out that the four columns of each group had typical load-axial shortening behaviour until a load between 550 kN to 600 kN, as shown in Fig. 7. Beyond this limit, enhancement in the bearing capacity of the specimens was noticed with increasing the steel tube thickness. In the non-deficient column with 5% rubberized concrete, increasing the steel tube thickness increased the ultimate bearing capacity of the column up to 20.57%. While in the similar specimens with 15% rubber content, the ultimate bearing capacity was increased up to 23.9%, compared to the reference specimens. In these two groups, no noticeable effect on the columns' ductility was noticed due to changing the tube thickness. However, it was observed that for the same steel tube thickness, the columns with RU15 concrete mix exhibited higher ductility and lower ultimate compressive strength than columns with RU5 concrete mix, as shown in Fig. 8.

In case of transversally (horizontal) deficiency in specimens with 5% rubber content (RuC 5%), increasing the steel tube thickness caused approximately uniform increase in ultimate load, as shown in Fig. 7 (c). In comparison with the steel tube with 2.5 mm thickness, the steel tube with 3 mm thickness exhibited higher ultimate compressive load by 4.3%, the steel tube with 3.5 mm thickness exhibited higher ultimate compressive load by 8.65% and the steel tube with 4 mm thickness exhibited higher ultimate compressive load by 14.48%. The equivalent specimens with 15% rubber content (RuC 15%), had increased percentages in the ultimate loads about 5.07%, 9.68% and 16.29% for columns with steel tube thicknesses of 3 mm, 3.5 mm and 4 mm, respectively. With the existence of longitudinal (vertical) deficiency in specimens with 5% rubber content, the increase in the steel tube thickness caused higher increase in the ultimate load of the studied columns. The increase corresponding to thickness variation were 6.2%, 12.2% and 18.5% with respect to the column with steel tube thickness of 2.5 mm. Very close increase values in the column capacities were noticed when 15% rubber content were used; 6.7%, 13.25% and 19.4%, as shown in Fig. 7 (f). The results demonstrated that the ultimate axial load bearing capacity of the analyzed columns decreased with increasing the D/t ratio, as illustrated in Fig. 9. Increasing the diameter to thickness ratio decreases the difference in the section capacities between the non-deficient and the deficient columns, regardless the concrete mix type, as shown in Fig. 9.

To evaluate the change in ductility with different steel tube thickness, ductility index (DI) was calculated as the ratio between the axial shortening at ultimate load to the axial shortening at yield. In general, the columns with concrete mix with 15% rubber content exhibited higher ductility compared to that with 5% rubber content. The value of the ductility index in specimens with vertical (longitudinal) deficiency were higher than that of specimens with horizontal (transversal) deficiency, as shown in Fig. 8. This might be due to the noticeable increase in the axial deformation accompanied with increasing the load until the ultimate load of the former columns.

Specimen	t [mm]	D/t	Rubber %	Deficiency	Strengthening type	NT	NL	$P_{u(FE)}$ (KN)	$\Delta_{u(FE)}$	DI
RU5-T2.5	2.5	50	5%	--	--	--	--	887	7.1	5
RU5-HL-T2.5	2.5	50	5%	T	--	--	--	870	7	7.1
RU5-VL-T2.5	2.5	50	5%	L	--	--	--	875	6.95	7.73
RU5-T3	3	42	5%	--	--	--	--	942	7.1	5
RU5-HL-T3	3	42	5%	T	--	--	--	907.5	6.35	6.68
RU5-VL-T3	3	42	5%	L	--	--	--	930	7.15	8.36
RU5-T3.5	3.5	36	5%	--	--	--	--	998.5	7.1	5
RU5-HL-T3.5	3.5	36	5%	T	--	--	--	945.3	6.15	6.47
RU5-VL-T3.5	3.5	36	5%	L	--	--	--	982	7.15	7.94
RU5-T4	4	32	5%	--	--	--	--	1069.5	7.1	5
RU5-HL-T4	4	32	5%	T	--	--	--	996	6.45	6.52
RU5-VL-T4	4	32	5%	L	--	--	--	1037	7.35	8.36
RU5-HL-G1T	2.5	50	5%	T	GFRP	1	--	983.8	7.5	10.7
RU5-HL-G1T1L	2.5	50	5%	T	GFRP	1	1	1066.2	11.1	15.85
RU5-HL-G2T	2.5	50	5%	T	GFRP	2	--	1118.7	11.1	16
RU5-HL-G2T1L	2.5	50	5%	T	GFRP	2	1	1163.3	11.1	15.85
RU5-HL-G3T	2.5	50	5%	T	GFRP	3	--	1192	10.3	14.71
RU5-HL-C1T	2.5	50	5%	T	CFRP	1	--	1113.9	6.95	9.92
RU5-HL-C1T1L	2.5	50	5%	T	CFRP	1	1	1183	7.5	10.71
RU5-HL-C2T	2.5	50	5%	T	CFRP	2	--	1281	6.7	9.57
RU5-HL-C2T1L	2.5	50	5%	T	CFRP	2	1	1363.2	7.1	10.14
RU5-HL-C3T	2.5	50	5%	T	CFRP	3	--	1449	6.7	9
RU5-VL-G1T	2.5	50	5%	L	GFRP	1	--	971	9.8	10.09
RU5-VL-G1T1L	2.5	50	5%	L	GFRP	1	1	988	7.1	10.44
RU5-VL-G2T	2.5	50	5%	L	GFRP	2	--	1066.6	9.5	13.57
RU5-VL-G2T1L	2.5	50	5%	L	GFRP	2	1	1084.8	8.7	12.43
RU5-VL-G3T	2.5	50	5%	L	GFRP	3	--	1113.9	8.3	11.5
RU5-VL-C1T	2.5	50	5%	L	CFRP	1	--	1093.7	5.35	9
RU5-VL-C1T1L	2.5	50	5%	L	CFRP	1	1	1168.1	7.75	10.33
RU5-VL-C2T	2.5	50	5%	L	CFRP	2	--	1112.1	3.95	5.26
RU5-VL-C2T1L	2.5	50	5%	L	CFRP	2	1	1225.3	5.35	7.13
RU5-VL-C3T	2.5	50	5%	L	CFRP	3	--	1197.3	3.95	5.26
RU15-T2.5	2.5	50	15%	--	--	--	--	824	7.5	6.8
RU15-HL-T2.5	2.5	50	15%	T	--	--	--	816	6.5	7.2
RU15-VL-T2.5	2.5	50	15%	L	--	--	--	827.8	7.15	7.78
RU15-T3	3	42	15%	--	--	--	--	895.3	7.5	6.8
RU15-HL-T3	3	42	15%	T	--	--	--	857.4	6.35	6.77
RU15-VL-T3	3	42	15%	L	--	--	--	883.2	7.3	8.47
RU15-T3.5	3.5	36	15%	--	--	--	--	948.2	7.1	6.8
RU15-HL-T3.5	3.5	36	15%	T	--	--	--	895	6.15	6.58
RU15-VL-T3.5	3.5	36	15%	L	--	--	--	937.5	7.55	8.18
RU15-T4	4	32	15%	--	--	--	--	1021.5	7.1	6.8
RU15-HL-T4	4	32	15%	T	--	--	--	949	6.45	6.64
RU15-VL-T4	4	32	15%	L	--	--	--	988.4	7.65	8.47
RU15-HL-G1T	2.5	50	15%	T	GFRP	1	--	927	8.7	12.43
RU15-HL-G1T1L	2.5	50	15%	T	GFRP	1	1	995	11	15.95
RU15-HL-G2T	2.5	50	15%	T	GFRP	2	--	1055.3	11.4	16.43
RU15-HL-G2T1L	2.5	50	15%	T	GFRP	2	1	1092.1	11.4	15.95
RU15-HL-G3T	2.5	50	15%	T	GFRP	3	--	1113.1	10	14.87
RU15-HL-C1T	2.5	50	15%	T	CFRP	1	--	1026.4	6.35	10.2
RU15-HL-C1T1L	2.5	50	15%	T	CFRP	1	1	1125.9	7.9	11.3
RU15-HL-C2T	2.5	50	15%	T	CFRP	2	--	1211.2	6.7	9.9
RU15-HL-C2T1L	2.5	50	15%	T	CFRP	2	1	1343	7.9	10.9
RU15-HL-C3T	2.5	50	15%	T	CFRP	3	--	1448	6.7	9.6
RU15-VL-G1T	2.5	50	15%	L	GFRP	1	--	900.2	6.15	8.2
RU15-VL-G1T1L	2.5	50	15%	L	GFRP	1	1	937.8	7.1	10.7
RU15-VL-G2T	2.5	50	15%	L	GFRP	2	--	1017	9.5	13.8
RU15-VL-G2T1L	2.5	50	15%	L	GFRP	2	1	1035	8.7	12.8
RU15-VL-G3T	2.5	50	15%	L	GFRP	3	--	1064	8.3	12
RU15-VL-C1T	2.5	50	15%	L	CFRP	1	--	1009	5.55	8.25
RU15-VL-C1T1L	2.5	50	15%	L	CFRP	1	1	1117.5	7.75	11
RU15-VL-C2T	2.5	50	15%	L	CFRP	2	--	1057.4	3.55	5.4
RU15-VL-C2T1L	2.5	50	15%	L	CFRP	2	1	1155.1	5.1	7.24
RU15-VL-C3T	2.5	50	15%	L	CFRP	3	--	1061.5	2.95	4.22

T: Transversal; NT: No. of layers in transverse direction; L: Longitudinal; NL: No. of layers in longitudinal direction

Table 4: Specimens details and results for the parametric study.

Strengthening using FRP sheets

Forty RuCFST columns were externally bonded by FRP Sheets. Two different fiber types were used in this study, Carbon FRP sheets and Glass FRP sheets. The sheets were utilized to strengthen deficient RuCFST columns, with either horizontal (transversal) or vertical (longitudinal) deficiencies. Five strengthening schemes were used for each deficiency type and each FRP sheet. The layouts included layer(s) being wrapped around the RuCFST column perpendicular to the load direction (transversely), and layer bonded parallel to the axial load (longitudinally). The five schemes were: one transversal layer denoted by (1T); one transversal layer and one longitudinal layer (1T1L); two transversal layers (2T); two transversal layers and one longitudinal layer (2T1L) and three transversal layers; as detailed in Tab. 4. The aforementioned dimensions of the steel tubes with D/t ratio of 50 were used in this investigation. The proposed strengthening schemes were applied on specimens with transverse and longitudinal deficiencies with both types of rubberized concrete (with 5% and 15% crumb rubber content).

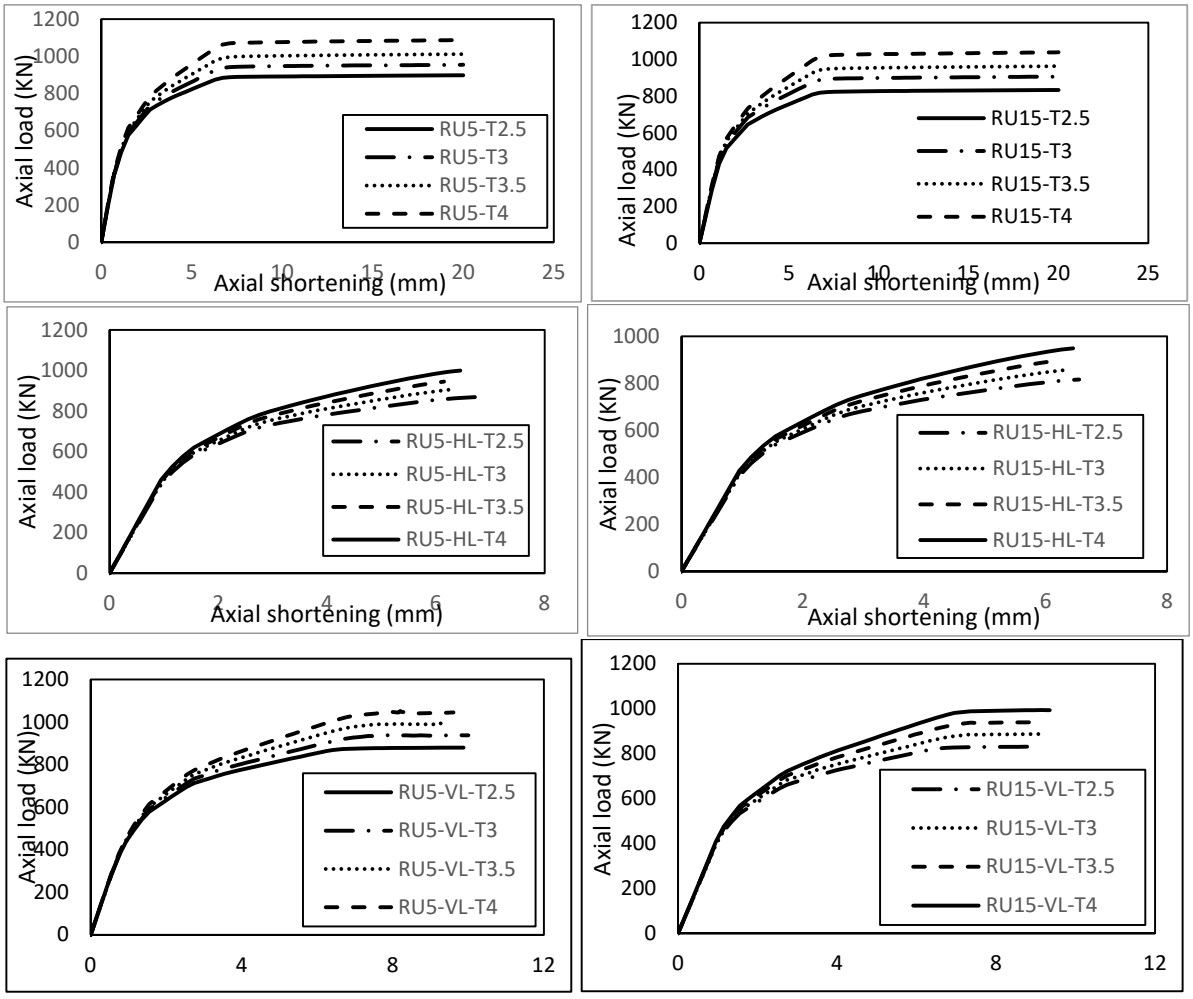

Figure 7: Axial load- axial shortening for specimens with various steel tube thickness.

Glass Fiber Reinforced Polymer (GFRP) Sheets

Composite columns filled with rubberized concrete with rubber replacements percentages of 5% and 15% were strengthened using the techniques mentioned above. For lateral strengthening schemes, increasing the number of GFRP layers increased the ultimate compressive load with increasing the number of layers. Using two and three transversal GFRP layers increased the ultimate compressive strength by 13.7% and 21.16%, respectively, compared to that with one GFRP layer. It was observed that the orientation of the layers had its effect on that increase in the ultimate compressive load. In comparison with the column strengthened with one transversal GFRP layer, using one transversal layer in addition to one longitudinal GFRP layer increased the ultimate compressive strength by 8.4%. Using two transversal layers in addition to

one longitudinal GFRP layer increased the ultimate compressive strength by 18.2%. These results indicated that using transversal layers in strengthening was more effective in increasing ultimate bearing capacity than using a combination of transversal and longitudinal layers with the same number of layers, as shown in Fig. 10 (a). Similar trend was observed in columns with 15% rubber content, as shown in Fig. 10 (b). In comparison with the column strengthened with one transversal GFRP layer, using one transversal layer in addition to one longitudinal GFRP layer increased the ultimate compressive strength by 7.3% while using two transversal GFRP layers increased the ultimate compressive strength by 13.8%. Using two transversal layers in addition to one longitudinal GFRP layer increased the ultimate compressive strength by 17.8% while using three transversal GFRP layers increased the ultimate compressive strength by 20% that led to the result that existence of transversal layers in strengthening was more effective than using a combination of transversal and longitudinal layers with the same number of layers. However, adding one longitudinal layer to transversal layers increased the ductility index of the specimen, as shown in Fig. 11. Using more than two GFRP layers led to a decrease in ductility index.

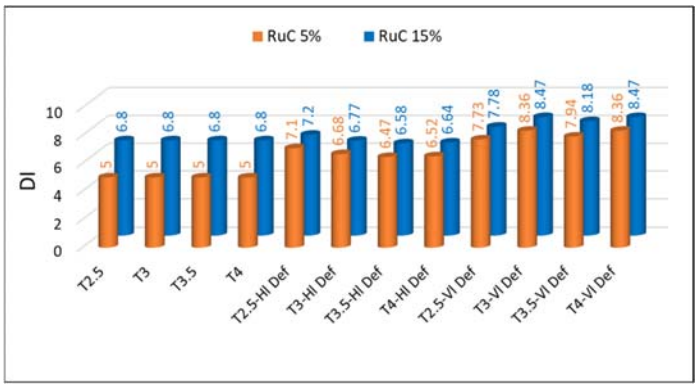

Figure 8: Ductility index of the specimens with various steel tube thickness.

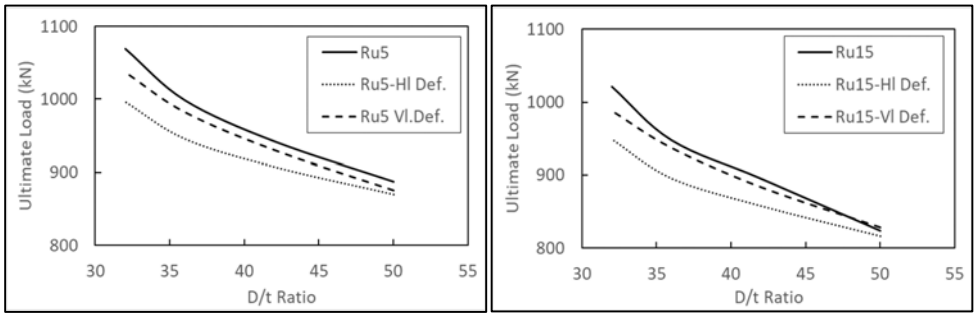

(a) (b)

Figure 9: Ultimate bearing capacity of the specimens with various steel tube thickness; (a) RU5 CFST, (b) RU15 CFST.

Strengthening specimens with longitudinal deficiency increased the ultimate bearing capacity, as shown in Fig. 10 (c). It was observed that the orientation of the layers was impressive in enhancing the deficient columns behaviour. Using two GFRP layers in transversal direction increased the ultimate compressive strength by 9.8%, while using one transversal layer and one longitudinal GFRP layer increased the ultimate compressive strength by only 1.7%, In comparison with the column strengthened with one transversal GFRP layer. Three transversal GFRP layers increased the ultimate compressive strength by 14.7%, while using two transversal layers in addition to one longitudinal GFRP layer increased the ultimate compressive strength by only 11.7%. These results indicate that with existence of vertical deficiency, transversal GFRP layers in strengthening was more effective than using a combination of transversal and longitudinal layers with the same number of layers. The equivalent columns with 15% rubber particles replacement showed better performance. In comparison with the column strengthened with one transversal GFRP layer, using two transversal GFRP layers increased the ultimate compressive strength by 12.9%. However, using one transversal layer in addition to one longitudinal GFRP layer increased the ultimate compressive strength by only 4.17%. Three transversal GFRP layers increased the ultimate compressive strength by 18.2%, whereas two transversal layers in addition to one longitudinal GFRP layer increased the ultimate compressive strength by 14.9%.

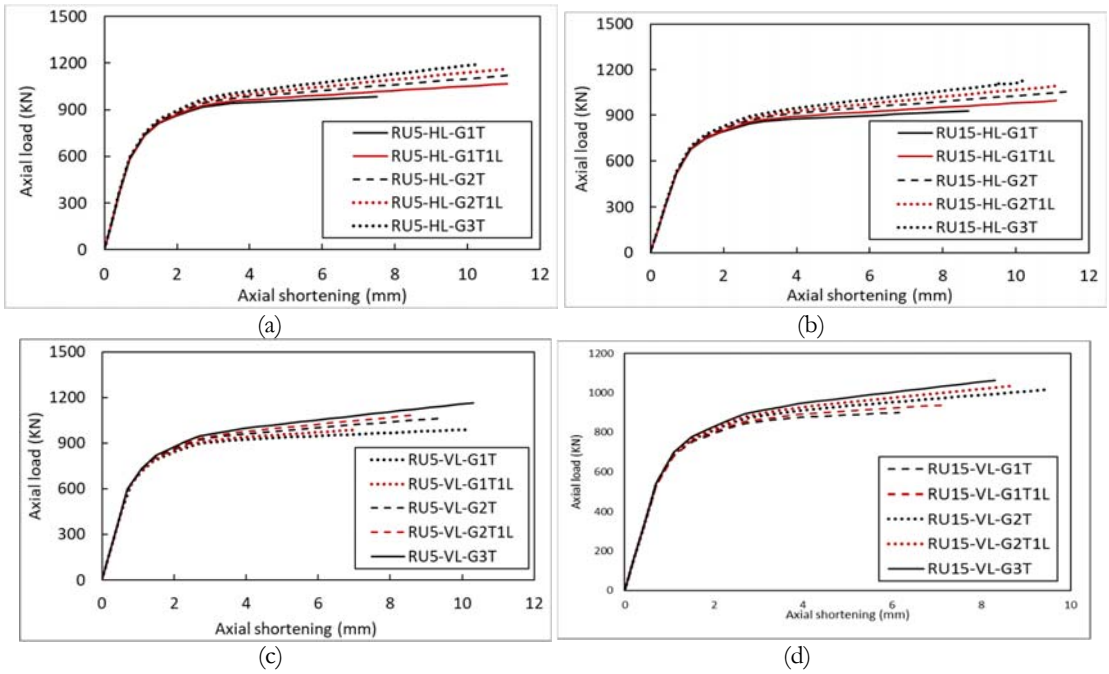

Figure 10: Axial load-axial shortening curves of specimens strengthened with various number and orientation of GFRP sheets; (a) RU5-HL-G CFST, (b) RU15-HL-G CFST, (c) RU5-VL-G CFST and (d) RU15-VL-G CFST.

The increase in the ultimate capacity of the columns was accompanied with contra verse effect on the column ductility, as shown in Fig. 11. Adding one longitudinal layer to the transversal layer increased the ductility index by 30.5% while using two transversal layers increased the ductility index by 68.3%. Using two transversal layers in addition to one longitudinal layer increased the ductility index by 56.1% and using three transversal layers increased the ductility index by 46.3% in comparison with using only one transversal layer as shown in Fig. 11. Using of two transversal layers was the most effective in enhancing the ductile behavior. The ductility index decreased with the increase in number of strengthening layers more than two transversal layers. Similar behaviour with slightly different enhancement percentages were noticed in specimens with 15% RuC, as illustrated in Fig. 11.

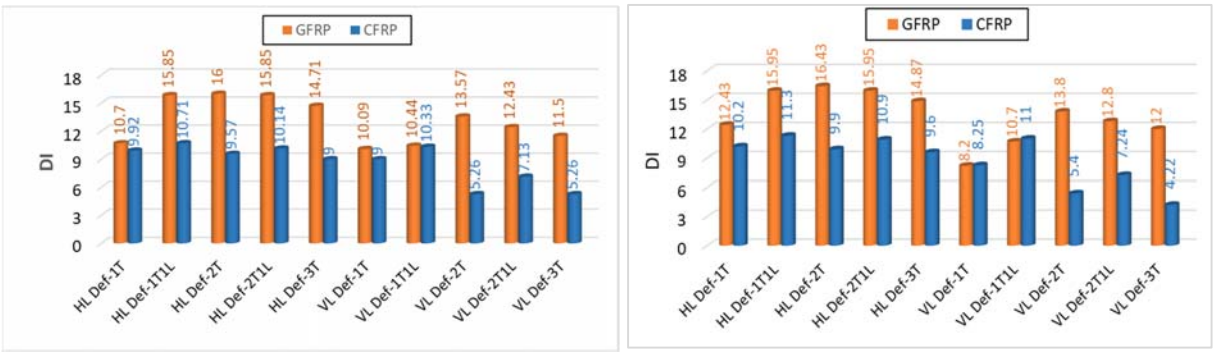

Figure 11: Ductility index for specimens strengthened with various number and orientation of FRP sheets; (a) RuC 5%, (b) RuC 15%.

Carbon Fiber Reinforced Polymer (CFRP) Sheets

CFRP sheets had a higher impact on the load carrying capacity of RuCFST columns than GFRP sheets. The increase in the ultimate compressive strength of the studied columns with 5% rubber replacement and horizontal deficiency was about 15% and 30% when using two and three transversal CFRP layers, respectively, in comparison with the column strengthened with one transversal CFRP layer. The orientation of the layers was effective in enhancing the ductility of the columns. However, the increase in the load carrying capacity was not as high as when using the same number of CFRP layers in the transverse direction. Using one transversal layer in addition to one longitudinal CFRP layer increased the ultimate

compressive strength by only 6.2%. While using two transversal layers in addition to one longitudinal CFRP layer increased the ultimate compressive strength by 22.4%. The same attitude was noticed in columns with 15% rubber replacement, as shown in Fig. 12. The increase in ultimate compressive strength in columns wrapped with two and three layers of CFRP sheets reached 18% and 41%, respectively. Using one longitudinal layer in addition to one and two transversal layers increased the ultimate compressive strength by 9.7% and 30.8%, respectively.

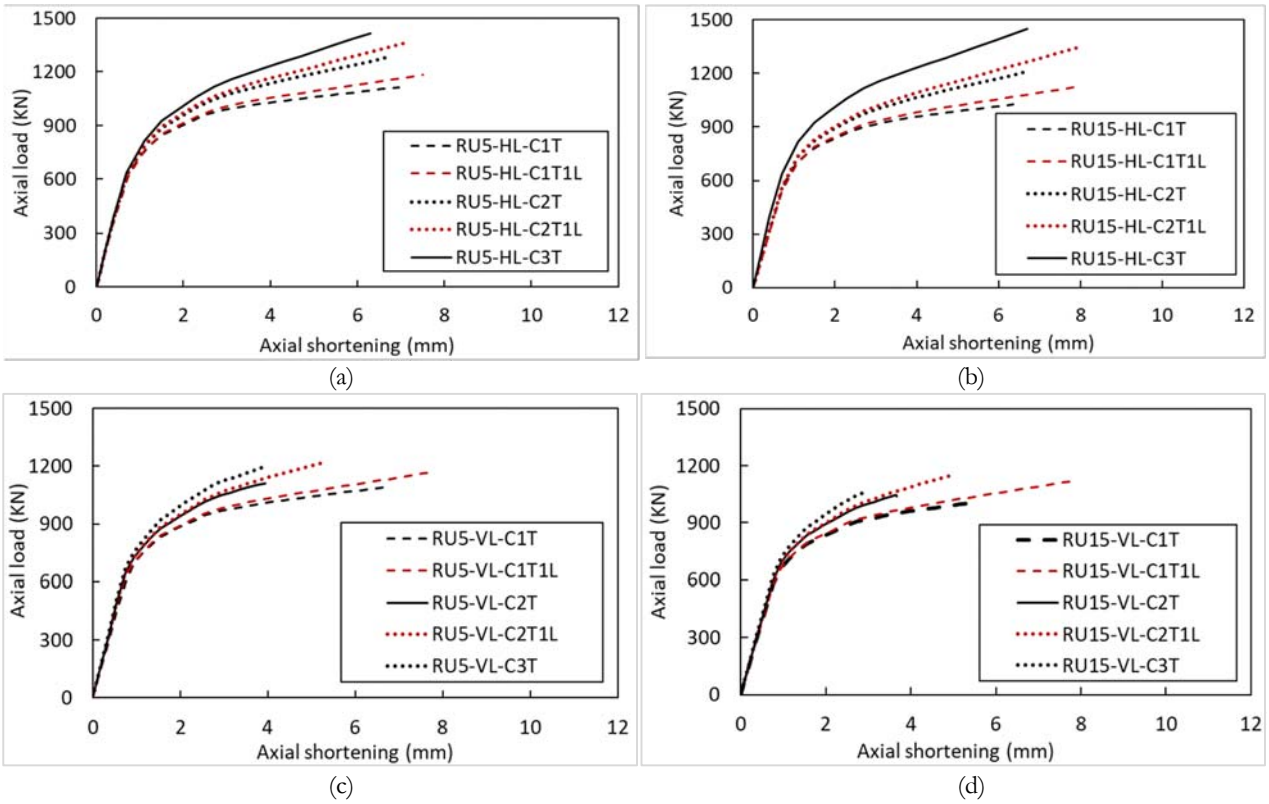

Figure 12: Axial load-axial shortening curves of specimens strengthened with various number and orientation of CFRP sheets; (a) RU5-HL-C CFST, (b) RU15-HL-C CFST, (c) RU5-VL-C CFST and (d) RU15-VL-C CFST.

RuCFST columns with vertical deficiency were strengthened with the aforementioned five patterns as well. Using three transversal CFRP layers increased the ultimate compressive strength by 9.4% and 5.2%, respectively in columns with 5% and 15% rubber content. However, using the same number of CFRP layer with different orientations; two transverse layers and one longitudinal layer; resulted in increase the strength enhancement by 12% and 14.5%, respectively, as shown in Fig. 12. This shows that existence of longitudinal layer in addition to transversal layers in strengthening was more effective than using only transversal layers with the same number of layers in specimens with vertical deficiency. This might be because of the effectiveness of longitudinal layer in resisting the local outward buckling at the deficiency location. Moreover, it was observed that the existence of longitudinal layer led to an increase in ductility index which decreased with the increase in number of transversal layers added to one longitudinal layer. Using two and three transversal layers led to a decrease in the ductility index in comparison with using only one transversal layer as shown in Fig. 11. This decrease might be because of high confinement provided by the CFRP sheets. The highest ductility was achieved in specimen with one transversal layer in addition to one longitudinal CFRP layer.

Conclusion

A three-dimensional nonlinear finite element model of non-deficient and transversally/longitudinally deficient short rubberized concrete filled steel tubular (RuCFST) columns was proposed in this paper. The model was verified against some available experimental results. To restore the loss in the column bearing capacity, the columns were strengthened with two types of FRP sheets under axial compressive load. Five different strengthening schemes were

analyzed. Increasing the steel tube's thickness was considered as well. Based on the results of the study, the following conclusions can be drawn:

- Increasing rubber content in the deficient RuCFST columns led to an increase in the ductile behavior and a decrease in ultimate bearing capacity.
- In bare RuCFST columns, local buckling at the deficiency corners caused noticeable decrease in the column strength and premature failure. This was controlled by the bonded layers of the FRP sheets wrapped around the columns.
- The axial capacity of the RuCFST columns increased by decreasing the diameter/thickness ratio of the steel tube. However, no significant enhancement was noticed in the ductile behavior of the columns due to this change in the D/T ratio.
- Increasing GFRP layers had its effect on columns behaviour. In case of horizontally and vertically deficient specimens, ultimate load increased with the increase of GFRP layers. Using three transversal GFRP layers increased the ultimate load up to 21.16% and 18.2%, respectively, compared to using one transversal layer. For horizontally and vertically deficient RuCFST columns, using two transversal layers achieved the highest ductile behaviour with increase up to 49.5% and 68.3%, respectively, compared to using one transversal layer.
- Significant Higher increase in the ultimate load capacity was recorded in case of CFRP strengthening. Horizontally deficient RuCFST columns showed enhancement up to 41%. Strengthening vertical deficiency showed lower enhancement reached 14.5%.
- Using two transversal GFRP layers achieved the highest ductility index with good increase in ultimate bearing capacity in case of transversally and longitudinally deficient specimens. Using one transversal layer in addition to one longitudinal CFRP was the best strengthening pattern using CFRP and achieved the highest ductile behaviour with good enhancement in ultimate load.
- Strengthening deficient RuCFST columns using GFRP sheets showed better ductility but lower bearing capacity compared to those strengthened using CFRP sheets. For all strengthened RuCFST columns under axial load, it was remarkably observed that strengthening the whole deficient columns with FRP sheets enhanced the ductility of the columns compared with the non-strengthened columns.

REFERENCES

[1] Schneider, S.P., 1998. Axially loaded concrete-filled steel tubes, J. of Structural Engineering, 124(10), pp. 1125-1138. DOI: 10.1061/(ASCE)0733-9445(1998)124:10(1125).

[2] Sundarraja, M. C. and Prabhu, G. G. (2012). Experimental study on CFST members strengthened by CFRP composites under compression, J. Constructional Steel Research, 72, pp. 75-83. DOI: 10.1016/j.jcsr.2011.10.014.

[3] Lu, Y., Li, N. and Li, S. (2014). Behavior of FRP-confined concrete-filled steel tube columns, Polymers, 6(5), pp. 1333-1349. DOI: 10.3390/polym6051333.

[4] Shen, Q., Wang, J., Wang, J. and Ding, Z. (2019). Axial compressive performance of circular CFST columns partially wrapped by carbon FRP, J. Constructional Steel Research, 155, pp. 90-106. DOI: 10.1016/j.jcsr.2018.12.017.

[5] Prabhu, G.G. and Sundarraja, M.C., 2013. Behaviour of concrete filled steel tubular (CFST) short columns externally reinforced using CFRP strips composite. Construction and Building Materials, 47, pp.1362-1371. DOI: 10.1016/j.conbuildmat.2013.06.038

[6] Prabhu, G.G., Sundarraja, M.C. and Kim, Y.Y., 2015. Compressive behavior of circular CFST columns externally reinforced using CFRp composites. Thin-Walled Structures, 87, pp.139-148. DOI: 10.1016/j.tws.2014.11.005.

[7] Alam, M.I., Fawzia, S., Zhao, X.L., Remennikov, A.M., Bambach, M.R. and Elchalakani, M., 2017. Performance and dynamic behaviour of FRP strengthened CFST members subjected to lateral impact. Engineering Structures, 147, pp.160-176. DOI: 10.1016/j.engstruct.2017.05.052.

[8] Deng, J., Zheng, Y., Wang, Y., Liu, T. and Li, H., 2017. Study on axial compressive capacity of FRP-confined concrete-filled steel tubes and its comparisons with other composite structural systems. International Journal of Polymer Science, 2017. DOI: 10.1155/2017/6272754.

[9] Liu, J.P., Xu, T.X., Wang, Y.H. and Guo, Y., 2018. Axial behaviour of circular steel tubed concrete stub columns confined by CFRP materials. Construction and Building Materials, 168, pp.221-231. DOI: 10.1016/j.conbuildmat.2018.02.131.

[10] Na, L., Yiyan, L., Shan, L. and Lan, L., 2018. Slenderness effects on concrete-filled steel tube columns confined with CFRP. Journal of Constructional Steel Research, 143, pp.110-118. DOI: 10.1016/j.jcsr.2017.12.014.

[11] Reddy, S.V.B. and Sivasankar, S., 2020. Axial Behaviour of Corroded CFST Columns Wrapped with GFRP Sheets—An Experimental Investigation. In Advances in Structural Engineering (pp. 15-28). Springer, Singapore. DOI: 10.1007/978-981-15-4079-0_2.
[12] Cao, S., Wu, C. and Wang, W., 2020. Behavior of FRP confined UHPFRC-filled steel tube columns under axial compressive loading. Journal of Building Engineering, p.101511. DOI: 10.1016/j.jobe.2020.101511
[13] Tang, H., Chen, J., Fan, L., Sun, X. and Peng, C., 2020. Experimental investigation of FRP-confined concrete-filled stainless steel tube stub columns under axial compression. Thin-Walled Structures, 146, p.106483. DOI: 10.1016/j.tws.2019.106483
[14] Ghaemdoust, M. R., Narmashiri, K. and Yousefi, O. (2016). Structural behaviors of deficient steel SHS short columns strengthened using CFRP, J. Construction and Building Materials, 126, pp. 1002-1011. DOI: 10.1016/j.conbuildmat.2016.09.099.
[15] Karimian, M., Narmashiri, K., Shahraki, M. and Yousefi, O. (2017). Structural behaviors of deficient steel CHS short columns strengthened using CFRP, J. Constructional Steel Research, 138, pp. 555-564. DOI: 10.1016/j.jcsr.2017.07.021.
[16] Fawzy, H. M., Mustafa, S. A. A. and Elshazly, F.A. (2020). Rubberized concrete properties and its structural engineering applications – An overview, J. EIJEST, Vol. 30, 2020.
[17] Jiang, Y., Silva, A., Castro, J.M. and Monteiro, R., 2015. Experimental assessment of the behaviour of rubberized concrete filled steel tube members. International Conference on Behavior of Steel Structures in Seismic Areas, Shanghai, China. https://www.researchgate.net/profile/Antonio_Silva51/publication/303372060_Experimental_assessment_of_the_behaviour_of_rubberized_concrete_filled_steel_tube_members/links/573ee30f08ae9f741b320c17/Experimental-assessment-of-the-behaviour-of-rubberized-concrete-filled-steel-tube-members.pdf
[18] Duarte, A. P. C., Silva, B. A., Silvestre, N., De Brito, J., Júlio, E. and Castro, J. M. (2016). Tests and design of short steel tubes filled with rubberised concrete, J. Engineering Structures, 112, pp. 274-286. DOI: 10.1016/j.engstruct.2016.01.018.
[19] Abendeh, R., Ahmad, H. S. and Hunaiti, Y. M. (2016). Experimental studies on the behavior of concrete-filled steel tubes incorporating crumb rubber, J. Constructional Steel Research, 122, pp. 251-260. DOI: 10.1016/j.jcsr.2016.03.022.
[20] Elchalakani, M., Hassanein, M.F., Karrech, A., Fawzia, S., Yang, B. and Patel, V.I., (2018). Experimental tests and design of rubberised concrete-filled double skin circular tubular short columns. In Structures, 15, pp. 196-210. DOI: 10.1016/j.istruc.2018.07.004.
[21] Dong, M., Elchalakani, M., Karrech, A., Hassanein, M.F., Xie, T. and Yang, B., 2019. Behaviour and design of rubberised concrete filled steel tubes under combined loading conditions. Thin-Walled Structures, 139, pp.24-38. DOI: 10.1016/j.tws.2019.02.031.
[22] ANSYS Release 19.2 Finite Element Analysis System, ANSYS Inc.
[23] Elshazly, F. A, (2020). Retrofitting of CFST columns using FRP composites, MSc thesis, Structural Engineering Department, Faculty of Engineering, Zagazig University.
[24] Liang, Q.Q. and Fragomeni, S. (2009). Nonlinear analysis of circular concrete-filled steel tubular short columns under axial loading, J. Constructional Steel Research, 65 (12), pp. 2186–2196. DOI: 10.1016/j.jcsr.2009.06.015.
[25] Liang, Q.Q. (2018). Analysis and design of steel and composite structures, CRC Press. DOI: 10.1201/9781315274843.
[26] Liang, Q.Q. (2011). High strength circular concrete-filled steel tubular slender beam-columns, Part I: Numerical analysis, J. Constructional Steel Research, 67 (2), pp. 164–171. DOI: 10.1016/j.jcsr.2010.08.006.
[27] Mander, J.B., Priestley, M.J.N. and Park, R. (1988). Theoretical stress–strain model for confined concrete, J. Structural Engineering, 114 (8), pp. 1804–1826. DOI: 10.1061/(ASCE)0733-9445(1988)114:8(1804).
[28] Tang, J., Hino, S., Kuroda, I. and Ohta, T. (1996). Modeling of stress–strain relationships for steel and concrete in concrete filled circular steel tubular columns, J. Steel Construction Engineering, 3 (11), pp. 35–46. DOI: 10.11273/jssc1994.3.11_35.
[29] Hu, H.T., Huang, C.S., Wu, M.H. and Wu, Y.M. (2003). Nonlinear analysis of axially loaded concrete-filled tube columns with confinement effect, J. Structural Engineering, 129 (10), pp. 1322–1329. DOI: 10.1061/(ASCE)0733-9445(2003)129:10(1322).
[30] Richart, F.E., Brandtzaeg, A. and Brown, R.L. (1928). A Study of the Failure of Concrete under Combined Compressive Stresses, Bulletin 185, Champaign, IL: University of Illinois, J. Engineering Experimental Station. http://hdl.handle.net/2142/4277.
[31] Duarte, A. P. C., Silva, B. A., Silvestre, N., De Brito, J., Júlio, E. and Castro, J. M. (2016). Finite element modelling of short steel tubes filled with rubberized concrete. J. Composite Structures, 150, pp. 28-40.

DOI: 10.1016/j.compstruct.2016.04.048.
[32] Bradford, M.A., Loh, H.Y. and Uy, B., (2002). Slenderness limits for filled circular steel tubes. J. Constructional Steel Research, 58(2), pp. 243-252. DOI: 10.1016/S0143-974X(01)00043-8.